Archives of Acoustics Vol. 48, No. 2, pp. 171–181 (2023), doi: 10.24425/aoa.2023.145232

Research Paper

Investigation of the Effect of Non-Flat Surfaces on the Performance of Perforated Acoustic Absorber

Zahra HASHEMI[(1)], Ali FAHIM[(2)*], Mohammad Reza MONAZZAM[(3)]

[(1)] *Behbahan Faculty of Medical Sciences*
Behbahan, Iran

[(2)] *School of Engineering Science, College of Engineering, University of Tehran*
Tehran, Iran

[(3)] *School of Public Health, Tehran University of Medical Sciences*
Tehran, Iran

*Corresponding Author e-mail: a.fahim@ut.ac.ir

(*received April 10, 2022; accepted December 12, 2022*)

In order to investigate the effect of the surface shape on the performance of perforated panels, three non-flat shapes were considered for perforated panel with their absorption performance compared with the usual shape of the (flat) perforated panel. In order to simulate the absorption coefficient of a non-flat perforated panel, the finite element method was implemented by the COMSOL 5.3a software in the frequency domain. Numerical simulation results revealed that all the shapes defined in this paper improve the absorption coefficient at the mid and high frequencies. A and B shapes had a higher performance at frequencies above 800 Hz compared to the flat shape. Also, shape C had a relative superiority at all frequencies (1–2000 Hz) compared to the reference shape; this superiority is completely clear at frequencies above 800 Hz. The maximum absorption coefficient occurred within the 400–750 Hz range. After determining the best shape in terms of absorption coefficient (shape C), a perforated panel of 10 m^2 using fiberglass fibers and desired structural properties was built, and then it was also subjected to a statistical absorption coefficient test in the reverberation chamber according to the standard. The results of the statistical absorption coefficient measurement showed that the highest absorption coefficient was 0.77 at the frequency of 160 Hz. Also, to compare the experimental and numerical results, these conditions were implemented in a numerical environment and the statistical absorption coefficient was calculated according to the existing relationships. A comparison of the numerical and laboratory results revealed acceptable agreement for these two methods in most frequency spectra, where the numerical method was able to predict this quantity with good accuracy.

Keywords: perforated acoustic absorber; surface shape; statistical absorption coefficient; reverberation chamber; finite element method.

1. Introduction

When a single-frequency plane wave collides with a rigid wall, a static wave with a pressure amplitude twice the pressure amplitude of the incident wave is generated due to boundary conditions on the wall surface. In other words, all the acoustic energy of the incident wave is reflected by the wall and remains in the medium. The use of absorbent materials can reduce the wave energy reflected from the wall. Perforated panels are one of the most common resonant absorbers used for sound control. This type of absorbers is widely used due to their adjustable mechanical properties and ease of processing. The unique physical properties of the perforated panels have led to their application in complex mechanical systems such as magnetic resonance scanners (MRI) (Li, Mechefske, 2010), cooling systems (Allam, Åbom, 2014), turbofan motor (Jing *et al.*, 2008), as well as many buildings (Yu *et al.*, 2016; 2017) and mufflers (Fuchs, Zha,

1997; 2006). The perforated panel is a plate consisting of a number of orifices with a specified diameter and spacing, which are positioned on a rigid wall at a certain distance. The orifices on the plate are interconnected and parallel similar to many Helmholtz resonators. When the frequency of the incident wave is close to the natural frequency, the air column formed in the orifices is strongly vibrated and collides with the back wall. Acoustic energy is converted to thermal energy due to inertia and adhesion effects, whereby the noise decreases.

A good absorber has an air-like resistance (for example, a resistance close to 1 and a resistance-to-reactance ratio greater than 1) and a reactance far lower than that of air. This reactance is achieved by giving space to the back of the perforated panel. In such a structure, the characteristics of the orifices and the air gap of the back of the plate affect the resonance frequency. With the proper selection of structural parameters, appropriate absorption can be achieved within the specific frequency range without the need for porous materials. The absence of common porous materials allows for a "clean" system that is more suitable for hospitals, food, and pharmaceutical industries, and microelectronics (Li, Mechefske, 2010). Although perforated panels have been considered an alternative to porous and fibrous absorbers, they have lower performance than porous materials in terms of both the absorption rate and the absorption range. Recent studies to enhance the efficiency of perforated absorbers have indicated the importance of this class of absorbers and their role in reducing noise in specific frequency ranges.

Wang *et al.* (2014) achieved maximum absorption at different frequencies by utilizing the space behind the perforated panel and creating chambers with different depths. These frequencies were proportional to the depth of each sub-chamber. Lee and Kwon (2004) increased the absorption coefficient significantly using multiple perforated panels. The use of absorbers on the back of the perforated panel is another way through which Hashemi *et al.* (2019) improved the absorption range and absorption rate by placing foams of varying current resistance and changing their layout. Some studies have also used the resonance of the micro-perforated structure itself, especially at low frequencies (Lee *et al.*, 2005; Chang *et al.*, 2010).

Few studies have looked at the apparent shape of adsorbent materials. For example, Chen *et al.* (2000) examined the effect of the shape of porous absorbers behind the micro-perforated plate. The authors examined simple, semicircular, concave, and triangular shapes and concluded that the form of porous absorbers definitely affects the absorption coefficient at some frequencies. Easwaran and Munjal (1993) studied the sound reflection coefficient from the foam edges using the Galerkin finite element method. Bolton and Green (1986) investigated the rates of adsorption coefficient and sound transmission loss in a panel composite structure by the finite element method. The results of both studies revealed that the porous materials with an edged shape improve the rates of absorption coefficient and the transmission loss in some frequency bands. Wang *et al.* (2019) conducted a study investigating the absorption properties of a corrugated perforated plate. For this purpose, a three-dimensional finite element model was used to estimate the absorption properties of the corrugated perforated plate. The results showed that the replacement of sinusoidal micro-perforated panel (MPP) changes the state of connection in the air-mass system; as a result, its absorption performance is different from that of flat MPP.

Wang and Liu (2020) showed in their study on corrugated micro-perforated panel absorber (MPPA) that when the wavelength of the sound wave is short, the absorption performance of corrugated MPP is better than that of the flat type, and at long wavelengths, there is no difference in the absorption rate of the two absorbers. Another finding of this study is better absorption performance at dip points (non-resonant frequencies) compared to the flat perforated absorption type, which can be used to control the resonance or reduce the accidental broadband noise in large spaces and buildings.

According to studies, the number of researches examining the surface shape of absorbers, especially perforated absorbers, is sparse. Thus, the main aim of this study is to investigate the effect of the surface shape of perforated absorbers on their absorption performance. Note that only three shapes are considered in this study and the results cannot be generalized for other shapes. The investigations in this study are conducted with two numerical finite element and experimental methods, which are described in more detail later. Regarding the article structure, theoretical and numerical adjustment sections are provided. The results of the numerical and experimental methods and the validation of the numerical method are presented in the following sections, and finally, the discussion and conclusions are presented.

2. Theoretical framework

The classical approach for such a system involves calculating the impedance of an orifice and then calculating the total impedance of the perforated panel according to the perforation percentage. The total impedance of the system depends on the perforation percentage, the diameter of the orifices, and the thickness of the panel. Impedance is a complex quantity with two real and imaginary terms:

$$Z_M = X + j\omega M. \tag{1}$$

The real part of the acoustic impedance X represents the energy propagation and viscous losses of the sound wave propagated through the orifices, and is known as resistance. The imaginary part of $j\omega M$ is called reactance and refers to the mass of air moving through the orifices. Obviously, the impedance depends on both the real and the imaginary terms, as well as other factors used depending on the model. Also, the shape of the orifices is assumed in a way that the heat-dissipated energy is insignificant compared to the viscous dissipated energy. There is no interaction between the orifices. If the orifices are too close to each other, such an assumption is not suitable for calculating the impedance and can be modified using the Fok function. Maa (1998) provided a well-known equation for determining the acoustic impedance of perforated panels:

$$Z_{M(\mathrm{MPP})} = \frac{\sqrt{2}\eta k}{\phi d} + \frac{j\omega\rho_0}{\phi} \cdot \left\{ \frac{0.85d}{\psi(\xi)} + t\left[1 - \frac{2}{k\sqrt{-j}} \frac{j_1\left(s\sqrt{-j}\right)}{j_0\left(k\sqrt{-j}\right)}\right]^{-1}\right\}, \quad (2)$$

where ρ_0 represents the density of air, ω is the angular frequency, and $j = \sqrt{-1}$ denotes imaginary numbers. Here $k = d\sqrt{\frac{\omega\rho_0}{4\eta}}$, d denotes orifice diameter, t is the panel thickness, j_0 and j_1 indicate the Bessel functions of first class and order 0 and 1, η represents the viscosity coefficient, ϕ is the porosity, and s is the perforation ratio in percentage, ψ is the Fok function obtained by the following equation:

$$\psi(\xi) = \left(1 - 1.40925\xi + 0.33818\xi^3 + 0.06793\xi^5 - 0.02287\xi^6 + 0.03015\xi^7 - 0.01641\xi^8 + ...\right)^{-1}, \quad (3)$$

where $\xi = 0.88d/b$, and b is the distance between the orifices. As mentioned, the perforated panels should have rigid backing wall with a certain distance to become a resonance absorber. The impedance of the perforated surface (Z_s) and the backspace is obtained from the following relation:

$$Z_s = Z_{M(\mathrm{MPP})} - j\rho_0 c_0 \cot\left(\frac{\omega D}{c_0}\right), \quad (4)$$

where D represents the distance from the back of the perforated panel to the solid wall, $Z_{M(\mathrm{MPP})}$ denotes the perforated panel impedance, and c_0 is the speed of sound in air. The absorption coefficient of the perforated absorber panel for the normal state is the ratio of the scattered wave pressure to the absorbed wave pressure obtained from the following relationship:

$$\alpha = 1 - \left|\frac{Z_s - \rho_0 c_0}{Z_s + \rho_0 c_0}\right|^2. \quad (5)$$

The oblique absorption coefficient can be obtained from the following equation:

$$\alpha_{\theta,\beta} = \frac{\iint\limits_{S_{\mathrm{Inlet}}} \mathrm{Re}\left[(j\varphi)\left[\frac{\partial\varphi}{\partial z}\right]^*\right] \mathrm{d}x\,\mathrm{d}y}{K_0(\cos\theta) L_x L_y}, \quad (6)$$

where L_x and L_y indicate the length and width of the plate, respectively, φ is the velocity potential, and $k_0 = \frac{\omega}{C_0}$ is the wave number in free space.

Finally, the absorption coefficient in the diffusion field can be written as follows:

$$\alpha_S = \frac{1}{2\pi}\int_0^{2\pi}\left(\int_0^{\pi/2} \alpha_{\theta,\beta}\sin 2\theta\,\mathrm{d}\theta\right)\mathrm{d}\beta, \quad (7)$$

where θ and β are the angles of elevation and azimuth, respectively.

3. Methods

3.1. Numeric adjustment

In order to simulate the absorption coefficient of a non-flat perforated panel, the finite element method was used by COMSOL 5.3a software in the frequency domain. The computational range included the space behind the perforated panel, the perforated panel itself, and the virtual channel. This software solves the wave equation by solving the Helmholtz equation in the frequency domain. Given the non-flat surface of the perforated panel, it is not possible to claim that the normal absorption coefficient is obtained if the angle of a sound wave is 0. Thus, in this study, the angle of the sound wave between two modes, 0 (minimum) and 90 (maximum), was considered 45 degrees. The modeling was done in a 3D environment based on drawing two cubes separated by a parabolic plane. The shape of the plate was determined using the specified equations. The upper cube corresponded to the virtual channel, while the lower cube corresponded to the volume behind the perforated panel. The acoustic field inside the virtual channel was connected to the space behind the plate through the perforated panel orifices. The length and width of the virtual channel and the back channel of the plate were 100 cm and 100 cm. Depending on the shape of the plates, the depth of the micro-perforated panel back was defined with the effective height and obtained by integrating the volume behind the perforated panel. The effective depth behind the perforated panel was assumed to be 10 cm. Rigid boundary conditions were considered for back-channel walls and periodic conditions at virtual channel boundaries. By applying the perforated boundary condition to the perforated panel, the acoustic impedance of the perforated panel relative to air was obtained according

to the Maa formula. The Dirichlet-to-Neumann boundary conditions (Keller, Givoli, 1989), applied to the virtual channel inlet, would allow the sound wave to pass through this boundary without reflection.

To investigate the effect of the surface shape of the perforated panel, three designs: A, B, and C, were selected for the perforated panel surface (Fig. 1). Factors to consider in this study were the simplicity of the designs in terms of drawing in software and the construction plus use phase as well as aesthetics and decoration issues. Simulations were performed within the frequency range of 1 to 2000 Hz. Structural properties such as orifice diameter, perforation percentage, and plate thickness in all shapes were constant at 1 mm, 0.016%, and 1 mm, respectively (Table 1). The tetrahedral mesh type and mesh sizes were chosen uniformly. In addition to the shapes mentioned, a flat shape was also used as a reference for comparison with the selected designs. The simulations of the absorption coefficient were also compared with the flat shape results. Finally, according to the simulation results, the best

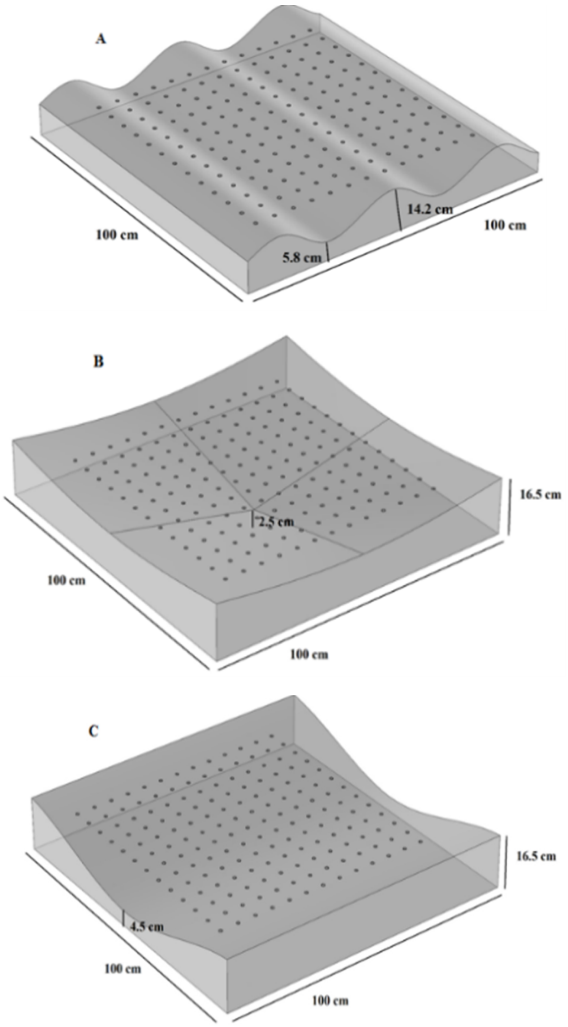

Fig. 1. Defined shapes for the perforated panel and their dimensions.

Table 1. Structural properties of the micro-perforated panel (numerical simulation).

Orifice diameter [mm]	Panel thickness [mm]	Effective height [mm]	Perforation ratio [%]
1	1	100	0.016

design in terms of absorption coefficient was chosen to construct at the required dimensions to determine the absorption coefficient in the reverberation chamber.

3.2. Measurement in the reverberation chamber

According to the results of the numerical solution, the best shape was selected in terms of the absorption coefficient. After making the desired piece (shape C – Fig. 1), the statistical absorption coefficient in the reverberation chamber was measured. The volume of the reverberation chamber was 100 m^3 and the roof area was 31.18 m^2. The diffusers installed in the chamber also helped disperse the sound wave and convert it into a completely diffuse place. Measurements were made in accordance with ISO 354: 2003 standard (ISO 354, 2003). According to this standard, the media dimensions to measure the statistical absorption coefficient must be at least 9 to 12 m^2. In this study, a perforated panel of 10 m^2 was built by putting 40 pieces of 50×50 cm together. The area of the surfaces and base of the panels was 11.92 m^2. Considering the economic constraints and problems, the molding method was used to fabricate the desired piece. To make the pieces lighter and easier to shape, 3 mm thick fiberglass and 3 mm orifices with a 0.5% perforation ratio (Table 2) perpendicular to the non-flat surface were used (Fig. 2). Note that the main focus of this study was the form factor study; thus, the selection of other

Fig. 2. Non-flat perforated panel (shape C) of 50×50 cm dimension.

Table 2. Structural properties of the micro-perforated panel (experimental simulation).

Orifice diameter [mm]	Panel thickness [mm]	Effective height [mm]	Perforation ratio [%]
3	3	100	0.5

parameters such as orifice diameter, perforation percentage, and thickness was not among the priorities of this study. There were also many limitations during the construction phase and the most applicable for these parameters was considered.

Different arrangements were proposed for this shape of the panel. Nevertheless, since the periodic boundary conditions were chosen for the virtual channel boundaries in this study (Fig. 3), suggesting that the sound wave conditions in the next panels can be repeated as before, the regular arrangement was considered at this stage. According to the standard, the sample arrangement should not be parallel to the walls of the room and should be half a meter from each wall. The sound was transmitted by a 12-dimensional loudspeaker in two locations, at frequencies of 100 to 5000 Hz in 1.3 octave steps in different directions, with the microphone manually positioned at five preset locations, and the experiments were repeated three times in each case. Finally, the average statistical absorption coefficients were obtained.

Fig. 3. Arrangement of the perforated panel in the reverberation chamber. The layout of the audio microphone and speaker.

For comparing the experimental method with the numerical methods, according to Eq. (7), the absorption coefficient at angles (θ = 0–90°, β = 0–180°) was calculated in the software separately; by averaging their values, the statistical absorption coefficient was obtained at 1.3 octave frequencies.

4. Results

4.1. Numerical results for selecting the best shape

The results of the finite element simulation were presented for the designs considered for the perforated panel compared to the flat shape (reference) and compared to each other. As mentioned earlier, the structural properties of the surface shape in all three shapes as well as the reference shape were very similar and the effective depth of all structures is 10 cm.

Figure 4 displays the simulation results of the absorption coefficient in the two flat (normal) perforated panels in A and reference shapes. The performance of both shapes at frequencies below 800 Hz was similar, but with increasing frequency, the perforated panel with a sinusoidal shape A performed better. At 240 Hz, there was a small peak in both diagrams, which could be due to the resonance of the chamber behind the perforated panel. Considering the similarity of properties such as orifice diameter, perforation percentage, and plate thickness in both samples, subsequent peaks occurred at both identical absorbers and at frequencies of 450 and 750, which is higher in absorber A with a negligible difference. Most of the absorption was observed within the frequency range of 450–800 Hz, with the performance of both absorbers declining above the frequency of 800 Hz and the absorption coefficient diminishing in the reference plate with a steeper slope.

As can be seen in Fig. 5, the perforated absorber B, which is actually an inverted pyramid scheme similar to absorber A, performs better at frequencies above 800 Hz compared to the flat shape. Meanwhile, it also functions better at frequencies below 800 Hz. For example, at the frequency of 400 Hz, it has an absorption coefficient of 0.82, while the absorption coefficient of the reference is 0.6. The next point to notice in this diagram is the higher resonance peak in the back chamber space at 240 Hz. Given the variable height of the back chamber as well as the higher height at

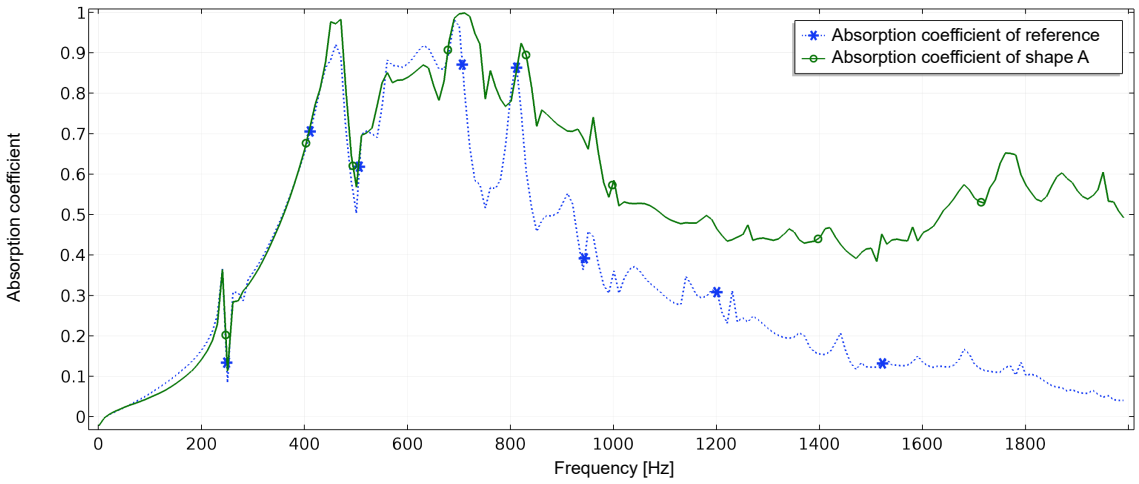

Fig. 4. Comparison of absorption coefficient in the two shapes of A and reference shape.

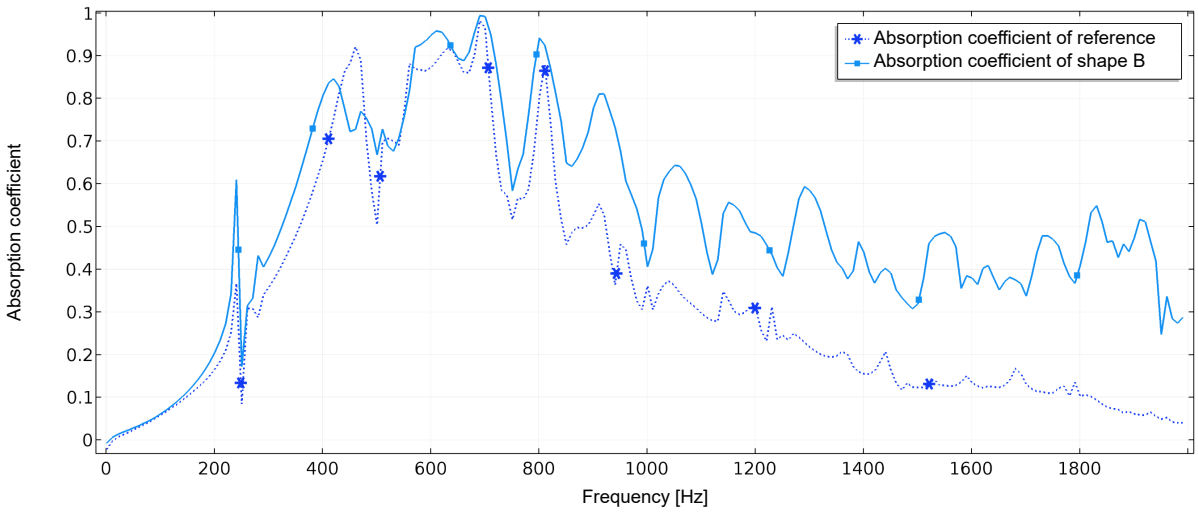

Fig. 5. Comparison of absorption coefficient in the two shapes of B and reference shape.

some points in absorber B, such a peak seems reasonable.

The results of shape C in Fig. 6 show relative superiority at all frequencies (1–2000 Hz) compared to the reference shape; this superiority is completely clear at frequencies above 800 Hz. The maximum absorption coefficient has occurred within the 400–750 Hz range.

Figure 7 well illustrates that at mid and high frequencies, the shapes defined in this study improve the performance of these absorbers, where the increased absorption rate by up to 3-fold is observed at some frequencies. Meanwhile, by designing and choosing the appropriate design and shape, the absorption pattern can be changed at lower frequencies, and a better absorption rate is achieved. The most important finding in these diagrams was the change in the absorption pattern in absorbers of unusual shape relative to the flat shape. On the other hand, further analysis showed that the changes in the perforated panel improved the absorption coefficient and wider absorption bandwidth. In terms of the absorption pattern, the absorption diagrams of these three designs differ due to reasons discussed below.

4.2. Results of statistical absorption coefficient in the experimental method (reverberation chamber)

Figure 8 shows the statistical absorption coefficient by the experimental method in the reverberation chamber. As can be seen, the highest absorption coefficient was observed at low frequencies (less than 250 Hz) and with a peak value of 0.77 at 160 Hz. Also, at 400 Hz a small peak was observed. What is significant in this graph is the acceptable absorption coefficient at low frequencies, which can be very important due to the low porosity of the absorbers in these areas.

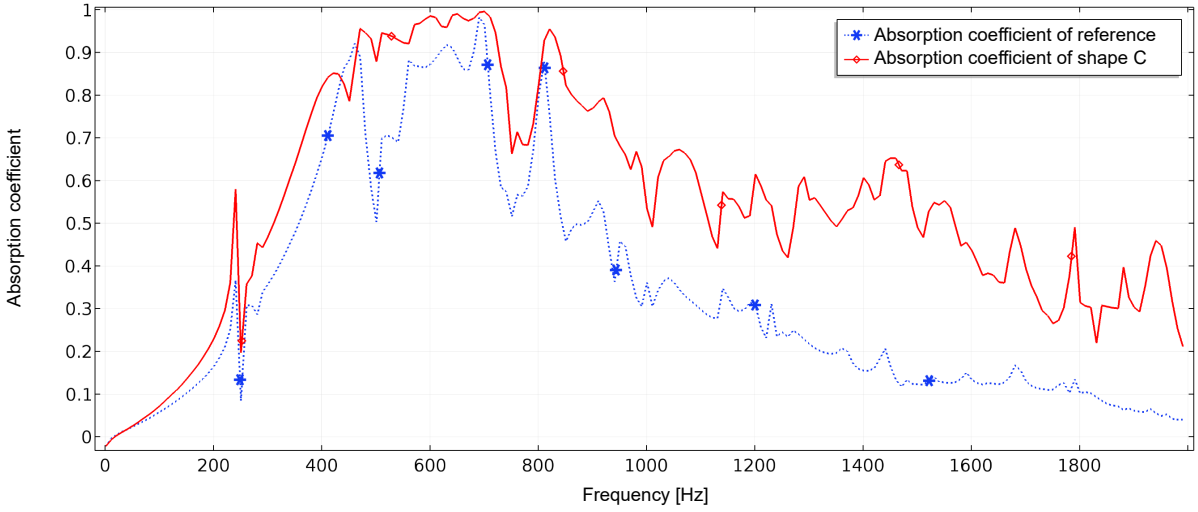

Fig. 6. Comparison of absorption coefficient in the two shapes of C and reference shape.

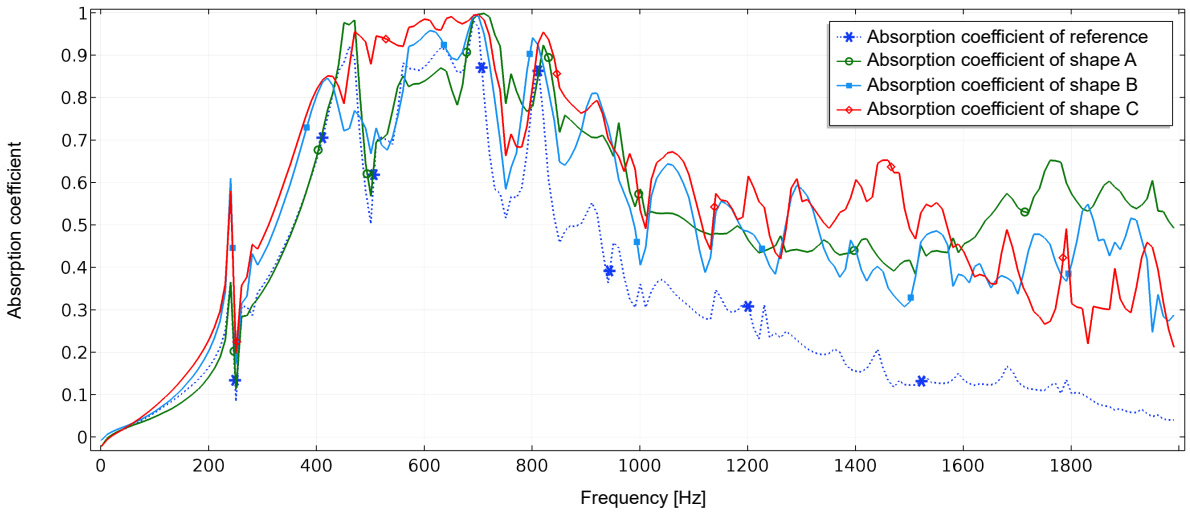

Fig. 7. Comparison of absorption coefficient in all studied shapes.

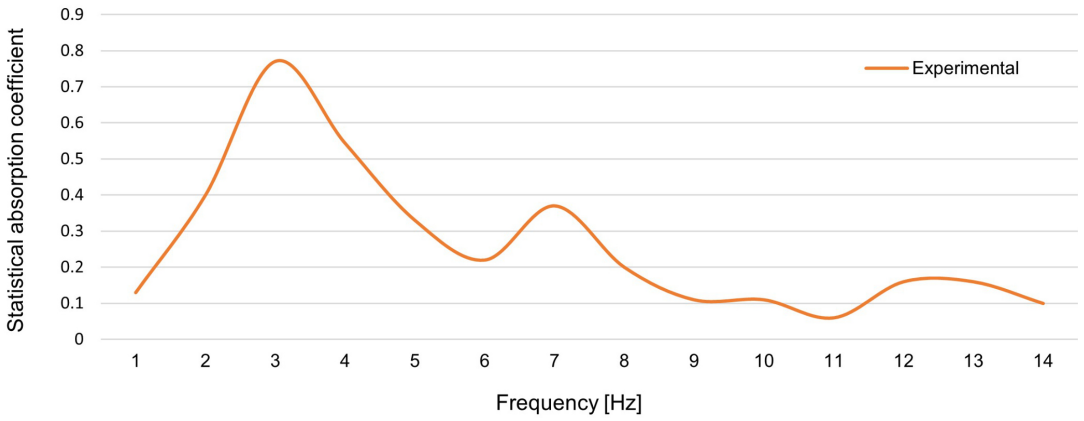

Fig. 8. Statistical absorption coefficient by the experimental method (shape C).

4.3. Comparison of the results of statistical absorption coefficient in FEM and experimental method

A comparison of the statistical absorption coefficient with experimental and numerical methods (Fig. 9) indicated the acceptable agreement of both methods in estimating this quantity. If the mismatch of the results at the frequency of 400 Hz is ignored, the absorption pattern is the same in both methods, and the numerical method simulated the results with acceptable accuracy. At some points, the experimental

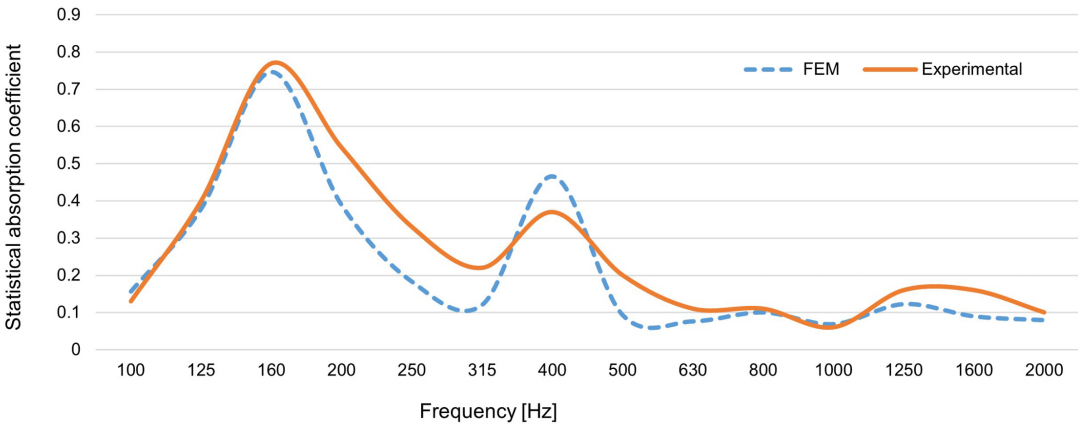

Fig. 9. Comparison of the statistical absorption coefficient with experimental and numerical methods.

absorption coefficient was higher than the value estimated by the numerical method, and the reasons are elaborated further.

5. Discussion

This study investigated the surface shape factor and its effect on the absorption performance of perforated panels. Initially, three simple shapes were defined as numerical tools in the software environment for the reasons mentioned, and with the same structural properties for these shapes, their absorption performance was compared to that of the flat shape. The results showed that the absorption performance increased at the mid and high frequencies, at least for the defined shapes. Also, at least in one of the shapes (C), there was a noticeable difference in the absorption coefficient at low frequencies, in addition to the high frequencies. In this study, the desired shape was constructed in 10 m^2 according to ISO 354 (2003) standard and its statistical absorption coefficient was measured in the reverberation chamber. Simultaneously, this quantity was simulated numerically.

Initially, these two issues should be explained:

– Why does the highest amount of absorption coefficient for all types of perforated absorbers occur at frequencies above 800 Hz?

With sound waves colliding with a hard and inflexible obstacle, the velocity of the particles will reach a maximum between a quarter and a third of the sound wavelength. If the absorber thickness is less than a quarter of the sound wavelength, its effect on absorption diminishes. This is the reason for acceptable absorption in the high-frequency spectrum using a thin absorber. As the shaping of the plates creates areas with variable heights, the maximum heights would lie within the range of 1/4 of the wavelength or close to this range, and therefore, better absorption is observed at higher frequencies compared to lower frequencies. The absorber depth must be very high to cover the range of 1/4 wavelength. In this regard, Wang *et al.* (2019) found that the absorption performance of a perforated wavy surface can be different from that of a flat perforated plate when the sound wavelength is less than the depth of air behind the perforated plate.

– Why did the absorption coefficient peak in Fig. 5 occur at 240 Hz for all types of perforated absorbers (three designs: A, B, and C)?

Different modes were tested to ensure no error in the numerical model, including the mesh size, mesh geometry, and different boundary conditions. In the present study, the rigid boundary condition was used for the chamber walls behind the perforated plate. This means that the chambers with an area of 100×100 cm^2 were separate from each other and might be subjected to the resonance phenomenon due to the dimensions at some frequencies. In the next step, the periodic boundary condition was considered instead of the rigid condition, with the periodic boundary condition signifying that the entire absorber area was continuous and not separated by hard walls. As a result, the shape area would be different from the previous state, and consequently, the resonance frequency would be different. Thus, the peaks of 240 Hz were eliminated with this change. According to the above reasons, it can be concluded that the presence of peaks at a frequency of 240 Hz was not due to a computational error, as these peaks disappeared by changing the boundary conditions. Also, the peaks related to the frequency of 240 Hz could be related to the resonance of the volume of the chamber behind the perforated plate.

In resonance absorbers, the air gap actually plays the spring role, whose value is controlled by the depth measure. Sound absorption in perforated panels is influenced by the resonance of the volume of vibrating air in the orifice and backspace. The change in the geometric configuration of the backspace can effectively alter the mass-spring coupling between the chamber and the perforated panel (Wang *et al.*, 2010). Also, the results of the study conducted by Lee and Lee (2007) on a flexible micro-perforated panel show this can be done by adjusting the curvature of the panel and thereby bringing the resonance frequencies closer to each other, the overall value of absorption coefficient increased. In irregular chambers, the real part of impedance contains not only the resistance of the perforated panel itself but also the acoustic energy transmitted from the chamber.

Further, the acoustic energy transmitted from these chambers has a different shape relative to the regular shape of the back chamber, which in turn, is closely related to the distortion of the shape of the acoustic modes in non-uniform chambers. In response to these changes, the resistance is not uniformly distributed on the surface of the perforated panel, and it alters the pattern of absorption. The perforated panels with a non-uniform back chamber have also been considered with multiple absorption features. The local absorption properties in non-uniform chambers are attributed to the variable impedance conditions. In this regard, we can refer to a study by Wang *et al.* (2010) by creating a trapezoidal chamber on the back of the micro-perforated panel and comparing it to the usual (rectangular) shape of the back of the micro-perforated panel. The authors concluded that the shape of the back chamber was very effective in the performance of the perforated absorbers and it made a significant difference to the efficiency of these types of absorbers. This improves the absorption performance and widens the absorption range. A number of researchers partitioned the backspace of a micro-perforated panel in the form of a honeycomb. The results showed that the unusual shape of the backspace increases the coupling between

the acoustic modes in the back chamber thus enhancing the absorption band (Sakagami *et al.* 2010; Yang, Cheng, 2016). These studies, in many ways, confirm the results of this study. Typically, in absorbers, several energy loss paths occur at the same time, such as reflection at the boundaries, deviation due to different speeds of sound propagation in separate materials, and air friction on the walls (Kulhavý *et al.*, 2018). When the soundwave hits a very flat surface on a plate, it will be reflected at the same angle. When the flat surface changes, i.e., it becomes shaped or angled, a part of the energy is propagated in a direction other than the reflection angle. This propagation and dispersion of the reflecting wave in different directions is called diffusion. Any non-flat surface can be considered a diffuser (Schroeder, 1975; 1979). The reflection mode or, in other words, the wave propagation in the back and front of the plate, depends entirely on the shape of the plate. One of the limitations of this study was a failure to deal with the contribution of each of these phenomena in changing the absorption pattern, yet definitely the complexity and interdependence of these factors have contributed to this.

In the remainder of this discussion, the phase difference caused by the discrepancy in the path length traveled by the waves entering the chamber behind the plate can also be investigated. The incident waves move a pressure wave to the bottom of the chamber, which is reflected upward after colliding with the bottom of the chamber. Considering the varying lengths of the traveled path in irregularly shaped chambers, phase difference occurs in these waves in the return path relative to each other. Whether these changes contribute to or attenuate the absorption is a complex phenomenon for which all factors should be examined. Nevertheless, it can be safely assumed that it changes the absorption pattern, which may also be associated with some of the changes in absorption curves. Also, the non-flatness of the perforated panel as the absorption surface means that the angle of the sound wave changes; obviously, the absorption coefficient depends on the angle of the radiation wave (Maa, 1998).

Changing the angle of the radiation wave can both support the absorption and reduce the absorption coefficient. Nevertheless, it is clear that when the surface is angled, the incident angle of the sound wave with the surface changes relative to its usual state. It may be argued that this would also contribute to the absorption in the shapes defined in this study.

The results of the statistical absorption coefficient in Fig. 8 show that the highest absorption rate was obtained at the low frequency of 160 Hz. Wave physics and the length of wavelength in this frequency region often render porous and fibrous absorbers ineffective in this area, and obtaining acceptable absorption coefficients in this region requires great weight constraints and thickness of these materials.

The most important advantage of resonance absorbers is the adjustable properties of these absorbers. Such a result is undoubtedly attributable to factors affecting the performance of perforated absorbers, including orifice diar, perforation percentage, backplate depth, and panel geometry as well as configuration. The results showed that the shape of the surface, and thus, the variable height behind the perforated panel have been effective for the reasons mentioned above. Considering the limitations of this study, we were not able to test the flat specimen with the structural properties of the specimen in the reverberation chamber. On the other hand, in the numerical environment, the laboratory test conditions were simulated and compared with the results of the reverberation chamber. The results revealed that the agreement between the two methods is acceptable, especially at low frequencies. The absorption coefficient in the experimental method was higher in most frequency spectra. Several mechanisms are effective in increasing the absorption coefficient in the experimental method, such as absorption by the frame around the sample. In the numerical method, only the surface of the absorber is computed in the calculations of the absorption coefficient, but this is inevitable in the reverberation chamber and there is a little extra absorption surface compared to the numerical conditions.

In addition, the vibration of the perforated panel and the edge effect can be mentioned. The effect of the edges is indeed the phenomenon of diffraction or sound wave refraction on the sample edges. The edge diffraction causes excess amounts of acoustic energy to enter into the perforated chamber, i.e., the absorption panel area is greater than the calculated value. Nevertheless, in most parts of Fig. 8, there is a good agreement between the two methods despite the differences. For example, at the frequency of 400 Hz, the absorption rate in the numerical method is higher than in the experimental method. Of course, despite the high precision of the pieces, there may be differences in some properties that are unavoidable in experimental methods.

6. Conclusion

In this study, three shapes were defined for the perforated panel, and their absorption performance was compared to the usual shape of the perforated absorbers at frequencies of 1–2000 Hz based on the numerical finite element method. According to the results obtained in this study, it can be stated that:

1) Sound absorption in perforated panels is influenced by the resonance of the volume of vibrating air in the orifices and backspace. The change in the geometric configuration of the backspace can effectively change the vibro-acoustic coupling between the chamber and the perforated panel, which in turn, changes the absorption pattern.

2) Chambers with unusual shapes have multiple and local absorptions due to their geometry. The local absorption properties in non-uniform chambers are attributed to the variable impedance conditions.
3) The way the wave reflects in the back and front of the plate depends entirely on the plate shape. In this study, the defined shapes changed the reflection of the waves as part of the energy dissipation path. The plate shape also caused the phase difference of the waves in the chamber due to the difference in path travel, affecting the efficiency of the absorbers.
4) In this study, only three shapes were examined where the selection of shapes was not scientifically based, and only their simplicity, constructability and applicability were considered. Also, the contribution of each phenomenon to energy dissipation was not estimated, so another study is required to cover these limitations.
5) The results of the absorption coefficient showed that the major absorption in this type of absorber occurred at low frequencies (160 Hz), which can be very important due to the low porosity of the absorbers in these areas.
6) There was an acceptable agreement on the statistical absorption coefficient between the numerical and experimental methods. It can be stated that the use of numerical methods such as finite element to predict the acoustic properties of different media, both in terms of speed of work and economic issues, can be very helpful.

Acknowledgments

This study was financially supported by the Tehran University of Medical Sciences & Health Services (Grant No.: 36052). Also, the first author would like to Mr. Farhad Taleei, Mr. Moghadami, Mr. Broghany, Mr. Karkhane, and Mr. Emami for their support and cooperation during this study.

References

1. Allam S., Åbom M. (2014), Fan noise control using microperforated splitter silencers, *Journal of Vibration and Acoustics*, **136**(3): 031017, doi: 10.1115/1.4027245.
2. Bolton J.S., Green E.R. (1986), Sound transmission through foam-lined double panel constructions, *The Journal of the Acoustical Society of America*, **79**(S1): S31–S31, doi: 10.1121/1.2023165.
3. Chang D., Liu B., Li X. (2010), An electromechanical low frequency panel sound absorber, *The Journal of the Acoustical Society of America*, **128**(2): 639–645, doi: 10.1121/1.3459838.
4. Chen W.-H., Lee F.-C., Chiang D.-M. (2000), On the acoustic absorption of porous materials with different surface shapes and perforated plates, *Journal of Sound and Vibration*, **237**(2): 337–355, doi: 10.1006/jsvi.2000.3029.
5. Easwaran V., Munjal M.L. (1993), Finite element analysis of wedges used in anechoic chambers, *Journal of Sound and Vibration*, **160**(2): 333–350, doi: 10.1006/jsvi.1993.1027.
6. Fuchs H.V., Zha X. (1997), Acrylic-glass sound absorbers in the plenum of the Deutscher Bundestag, *Applied Acoustics*, **51**(2): 211–217, doi: 10.1016/S0003-682X(96)00064-3.
7. Fuchs H.V., Zha X. (2006), Micro-perforated structures as sound absorbers – A review and outlook, *Acta Acustica united with Acustica*, **92**(1): 139–146.
8. Hashemi Z., Monazzam M.R., Fahim A. (2019), Estimation of sound absorption performance of complex perforated panel absorbers by numerical finite element method and examining the role of different layouts behind it, *Fluctuation and Noise Letters*, **18**(03): 1950013, doi: 10.1142/S0219477519500135.
9. ISO 354 (2003), Acoustics – Measurement of sound absorption in a reverberation room, *International Organization for Standardization*.
10. Jing X., Peng S., Sun X. (2008), A straightforward method for wall impedance eduction in a flow duct, *The Journal of the Acoustical Society of America*, **124**(1): 227–234, doi: 10.1121/1.2932256.
11. Keller J.B., Givoli D. (1989), Exact non-reflecting boundary conditions, *Journal of Computational Physics*, **82**(1): 172–192, doi: 10.1016/0021-9991(89)90041-7.
12. Kulhavý P., Samková A., Petru M., Pechociakova M. (2018), Improvement of the acoustic attenuation of plaster composites by the addition of short-fibre reinforcement, *Advances in Materials Science and Engineering*, **2018**: 7356721, doi: 10.1155/2018/7356721.
13. Lee D.H., Kwon Y.P. (2004), Estimation of the absorption performance of multiple layer perforated panel systems by transfer matrix method, *Journal of Sound and Vibration*, **278**(4–5): 847–860, doi: 10.1016/j.jsv.2003.10.017.
14. Lee Y.Y., Lee E.W.M. (2007), Widening the sound absorption bandwidths of flexible micro-perforated curved absorbers using structural and acoustic resonances, *International Journal of Mechanical Sciences*, **49**(8): 925–934, doi: 10.1016/j.ijmecsci.2007.01.008.
15. Lee Y.Y., Lee E.W.M., Ng C.F. (2005), Sound absorption of a finite flexible micro-perforated panel backed by an air cavity, *Journal of Sound and Vibration*, **287**(1–2): 227–243, doi: 10.1016/j.jsv.2004.11.024.
16. Li G., Mechefske C.K. (2010), A comprehensive experimental study of micro-perforated panel acoustic absorbers in MRI scanners, *Magnetic Resonance Materials in Physics, Biology and Medicine*, **23**(2): 177–185, doi: 10.1007/s10334-010-0216-9.

17. Maa D.Y. (1998), Potential of microperforated panel absorber, *The Journal of the Acoustical Society of America*, **104**(5): 2861–2866, doi: 10.1121/1.423870.

18. Sakagami K., Yamashita I., Yairi M., Morimoto M. (2010), Sound absorption characteristics of a honeycomb-backed microperforated panel absorber: Revised theory and experimental validation, *Noise Control Engineering Journal*, **58**(2): 157–162, doi: 10.3397/1.3294861.

19. Schroeder M.R. (1975), Diffuse sound reflection by maximum-length sequences, *The Journal of the Acoustical Society of America*, **57**(1): 149–150, doi: 10.1121/1.380425.

20. Schroeder M.R. (1979), Binaural dissimilarity and optimum ceilings for concert halls: More lateral sound diffusion, *The Journal of the Acoustical Society of America*, **65**(4): 958–963, doi: 10.1121/1.382601.

21. Wang C., Cheng L., Pan J., Yu G. (2010), Sound absorption of a micro-perforated panel backed by an irregular-shaped cavity, *The Journal of the Acoustical Society of America*, **127**(1): 238–246, doi: 10.1121/1.3257590.

22. Wang C., Huang L., Zhang Y. (2014), Oblique incidence sound absorption of parallel arrangement of multiple micro-perforated panel absorbers in a periodic pattern, *Journal of Sound and Vibration*, **333**(25): 6828–6842, doi: 10.1016/j.jsv.2014.08.009.

23. Wang C., Liu X. (2020), Investigation of the acoustic properties of corrugated micro-perforated panel backed by a rigid wall, *Mechanical Systems and Signal Processing*, **140**: 106699, doi: 10.1016/j.ymssp.2020.106699.

24. Wang C., Liu X., Lixi H. (2019), On the sound absorption performance of corrugated micro-perforated panel absorbers, [in:] *INTER-NOISE and NOISE-CON Congress and Conference Proceedings*, **259**(7): 2336–2347.

25. Yang C., Cheng L. (2016), Sound absorption of microperforated panels inside compact acoustic enclosures, *Journal of Sound and Vibration*, **360**: 140–155, doi: 10.1016/j.jsv.2015.09.024.

26. Yu X., Cui F.S., Cheng L. (2016), On the acoustic analysis and optimization of ducted ventilation systems using a sub-structuring approach, The *Journal of the Acoustical Society of America*, **139**: 279–289, doi: 10.1121/1.4939785.

27. Yu X., Lau S.K., Cheng L., Cui F. (2017), A numerical investigation on the sound insulation of ventilation windows, *Applied Acoustics*, **117**(Part A): 113–121, doi: 10.1016/j.apacoust.2016.11.006.